Migration of Cell under Couette Type Shear Flow Field between Parallel Disks: After and Before Proliferation

Shigehiro HASHIMOTO, Kosuke SHIMADA, Yuji ENDO

Biomedical Engineering, Department of Mechanical Engineering,
Kogakuin University, Tokyo, 163-8677, Japan
shashimoto@cc.kogakuin.ac.jp http://www.mech.kogakuin.ac.jp/labs/bio/

ABSTRACT

The effect of shear stress on the migration of each cell has been investigated at proliferation under the constant shear flow field *in vitro*. The culture medium was sandwiched with a constant gap between a lower stationary culture plate and an upper rotating parallel plate to make a Couette type of shear flow. Two types of cells were used in the test: C2C12 (mouse myoblast cell line), and HUVEC (Human Umbilical Vein Endothelial Cells). The shear stress (< 2 Pa) was continuously applied on cells for 24 hours in the incubator. The behavior of each cell was traced at the time-lapse images observed by an inverted phase contrast microscope placed in an incubator. The experiments show following results. HUVEC tends to migrate downstream. The tendency is remarkable after proliferation. Migration tends to be enhanced, when the adhesion area decreased at proliferation. Under the shear stress field (> 1 Pa), C2C12 tend to migrate to the lower shear stress area. The velocity of the migration is higher at HUVEC than C2C12. The experimental system is useful to study the quantitative relationships between the shear stress and the cell migration.

Keywords: Biomedical Engineering, Shear Stress, Migration, C2C12, HUVEC and Couette Flow.

1. INTRODUCTION

A biological cell migrates on the scaffold. The adsorption state affects the migration behavior. It is not easy to standardize the condition, after seeding cells. In the present study, the behavior of each cell is traced before and after proliferation. After proliferation, each cell newly initiates adhesion to the scaffold.

In several cases, the cell is exposed to the shear stress both *in vivo* and *in vitro*. The direction of the shear stress field can affect the direction of the migration [1, 2]. In the present study, the migration of each cell is traced in the shear stress field of the medium. The effect of the shear flow on the endothelial cells [3–10], which are exposed to the blood flow on the inner surface of the vessel wall [11–14], were investigated in many studies. In the previous study with the vortex flow [15] by the swinging plate *in vitro*, C2C12 made orientation perpendicular to the direction of the flow, although HUVEC made orientation along the streamline of the flow [15].

In the Poiseuille type of flow [16–18], the shear rate depends on the distance from the wall: highest at the wall. In the Couette type of flow, on the other hand, the shear rate is constant regardless of the distance from the wall [10, 19–23].

In the present study, an experimental system of the Couette type flow in the constant gap with a rotating disk [20, 21] has been used to apply the shear stress quantitatively on the cell during incubation at the microscopic observation *in vitro*. The effect of the shear stress field (< 2 Pa) on the cell has been studied about migration.

2. METHODS

Couette Type of Shear Flow Device

A Couette type of shear flow device has been designed: between a rotating disk and a stationary dish (Fig. 1). The medium is sheared between a rotating wall and a stationary wall. The stationary wall is the bottom of the culture dish (diameter 60 mm). In the device, the shear rate (γ) in the medium is calculated by Eq. (1).

$$\gamma = r\,\omega / d \tag{1}$$

In Eq. (1), ω is the angular velocity [rad s^{-1}], and d is the distance [m] between the wall of the moving disk and the wall of stationary plate. Between the parallel walls, d is constant. The shear rate (γ [s^{-1}]) in the gap between walls increases in proportion to the distance (r [m]) from the rotating axis. The angular velocity ω (< 22 rad s^{-1}) was controlled by the stepping motor. In the observation area of the microscope, r varies between 17 mm and 18 mm. The distance d, which was measured by the positions of the focus of the walls at the microscope, was between 0.28 mm and 0.56 mm. Variations on the shear rates (γ) between 0.6×10^3 s^{-1} and 1.3×10^3 s^{-1} are made in the present experiment by adjustment of these parameters. The shear stress (τ [Pa]) is calculated by the viscosity (η [Pa s]) of the medium.

$$\tau = \eta\,\gamma \tag{2}$$

Using the viscosity of the medium of 1.5×10^{-3} Pa s (measured by a cone and plate viscometer at 310 K), the variations of the shear stress τ have been calculated as the value between 0.9 Pa

and 2.0 Pa.

The rotating disk device is mounted on the stage of the inverted phase contrast microscope placed in the incubator. The device allows the microscopic observation of cells cultured on the stationary wall during exposure to the shear flow.

Cell Culture

Two types of cells were used in the test: C2C12 (mouse myoblast cell line originated with cross-striated muscle of C3H mouse, passage between eight and ten), and HUVEC (Human Umbilical Vein Endothelial Cells). Cells were cultured in D-MEM (Dulbecco's Modified Eagle's Medium): containing 10% decomplemented FBS (fetal bovine serum), and 1% penicillin/ streptomycin.

The cells were seeded on the dish at the density of 3000 cells/cm^2. To make adhesion of cells to the bottom of the culture dish, the cells were cultured for 24 hours in the incubator without flow stimulation (without rotation of the disk). After the pre-incubation for 24 hours without shear, the cells were continuously exposed to the shear flow field with the rotating disk for 24 hours in the incubator by the constant rotating speed of the disk. The constant speed was preset for each test to keep the designed constant shear stress field.

Measurement of Cell

The time-lapse microscopic image was taken every ten minutes during the cultivation. The contour of each cell adhered on the stationary plate of the scaffold was traced, and the projected two-dimensional area (S) at the image of each cell was calculated. The contour of each cell was approximated to ellipsoid (Fig. 2), and the centroid of each cell was used to track the migration of the cell. The flow direction was defined as x axis. The direction to the rotating axis was defined as y axis (Fig. 1). The migration velocity of each direction (v_x and v_y) was calculated using the time-lapse images. From these images, cells with the proliferation were picked up. At each cell, data (S, v_x, and v_y) were traced before and after two hours from the proliferation.

The behavior of cells adhering to the stationary wall surface under the shear stress is observed with a microscope. The experimental system allows continuous observation of cells during exposure to the shear flow in the incubator.

3. RESULTS

In Figs. 3−6, each mark corresponds to the traced area (S) of each cell. Fig. 3 shows the tracings of the area (S) of each cell before (Fig. 3a) and after (Fig. 3b) proliferation of C2C12 under the shear stress field of 1 Pa. Fig. 4 shows the tracings of the area (S) of each cell before (Fig. 4a) and after (Fig. 4b) proliferation of C2C12 under the shear stress field of 1.5 Pa. Fig. 5 shows the tracings of the area (S) of each cell before (Fig. 5a) and after (Fig. 5b) proliferation of HUVEC under the shear stress field of 0.9 Pa. Fig. 6 shows the tracings of the area (S) of each cell before (Fig. 6a) and after (Fig. 6b) proliferation of HUVEC under the shear stress field of 2 Pa. The area S decreases in forty minutes before proliferation, and increases in forty minutes after proliferation. For two hours before and after proliferation, the area S before proliferation is larger than that after proliferation. The area S tends to decrease under the shear stress field higher than 1 Pa.

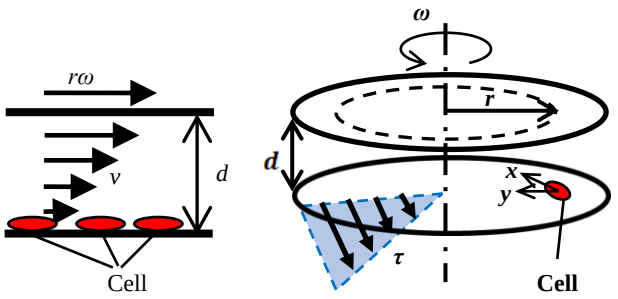

Fig. 1: Couette flow velocity distribution (v) between rotating (angular velocity ω) wall and stationary wall at r (radius) (distance d; left): shear stress (τ) on stationary wall (right).

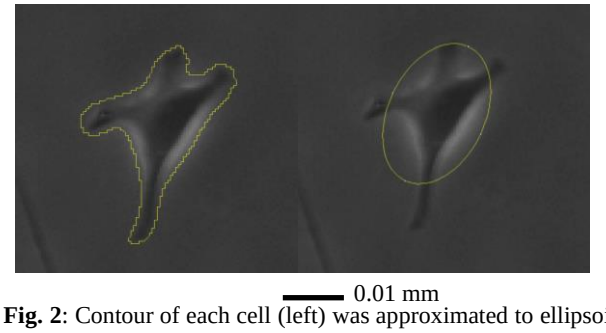

Fig. 2: Contour of each cell (left) was approximated to ellipsoid (right).

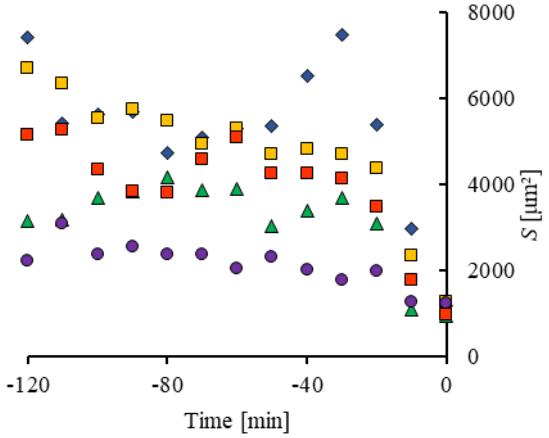

Fig. 3a: Tracings of area (S) before proliferation of C2C12 under shear stress field of 1 Pa.

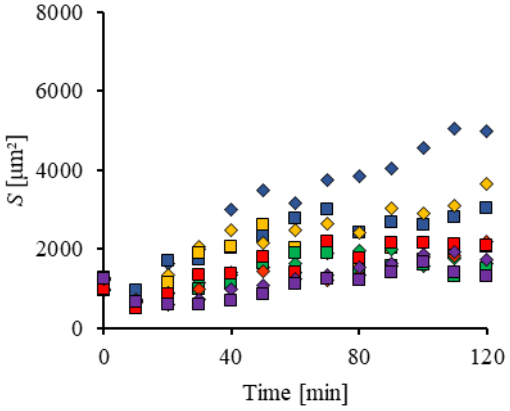

Fig. 3b: Tracings of area (S) after proliferation of C2C12 under shear stress field of 1 Pa.

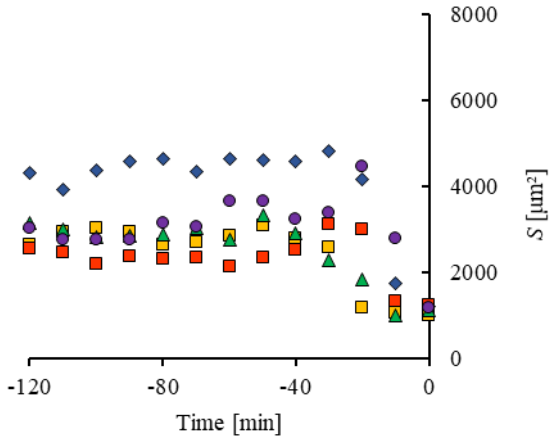

Fig. 4a: Tracings of area (*S*) before proliferation of C2C12 under shear stress field of 1.5 Pa.

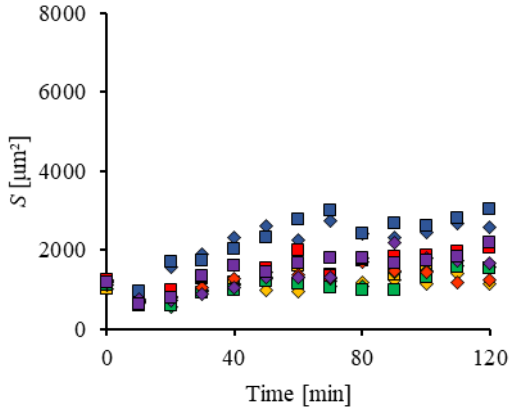

Fig. 4b: Tracings of area (*S*) after proliferation of C2C12 under shear stress field of 1.5 Pa.

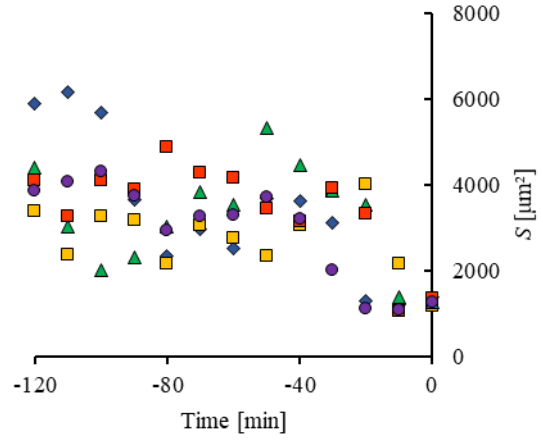

Fig. 5a: Tracings of area (*S*) before proliferation of HUVEC under shear stress field of 0.9 Pa.

Data of the migration velocities before (Fig. 7a) and after (Fig. 7b) proliferation of C2C12 under shear stress field of 1 Pa were collected in Fig. 7. Data of the migration velocities before (Fig. 8a) and after (Fig. 8b) proliferation of C2C12 under shear stress field of 1.5 Pa were collected in Fig. 8. Data of the migration velocities before (Fig. 9a) and after (Fig. 9b) proliferation of HUVEC under shear stress field of 0.9 Pa were collected in Fig. 9. Data of the migration velocities before (Fig. 10a) and after (Fig. 10b) proliferation of HUVEC under shear stress field of 2 Pa were collected in Fig. 10. The velocity of the migration tends to be biased downstream after proliferation. The tendency is remarkable in HUVEC, especially after proliferation (Figs. 9b & 10b). Under the higher shear stress field, C2C12 tend to migrate to the center of the rotating axis, which correspond to the lower shear stress area. The velocity of the migration tends to be higher at HUVEC than C2C12.

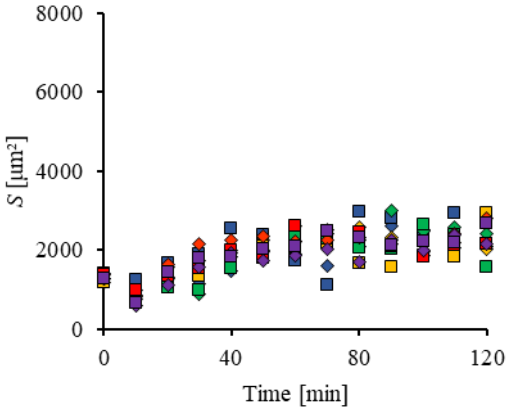

Fig. 5b: Tracings of area (*S*) after proliferation of HUVEC under shear stress field of 0.9 Pa.

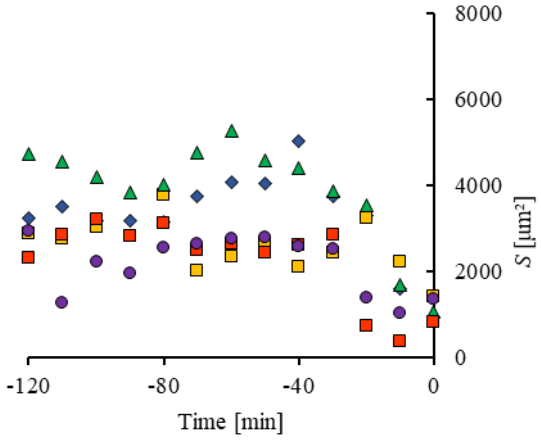

Fig. 6a: Tracings of area (*S*) before proliferation of HUVEC under shear stress field of 2 Pa.

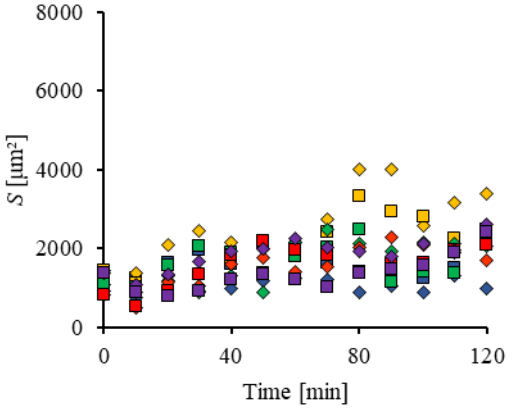

Fig. 6b: Tracings of area (*S*) after proliferation of HUVEC under shear stress field of 2 Pa.

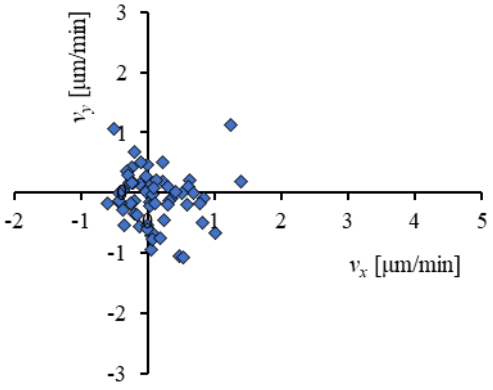

Fig. 7a: Migration velocity before proliferation of C2C12 under shear stress field of 1 Pa.

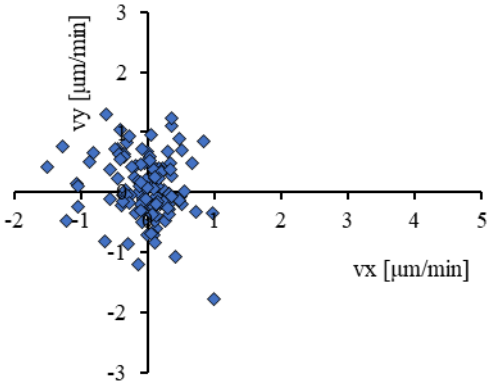

Fig. 7b: Migration velocity after proliferation of C2C12 under shear stress field of 1 Pa.

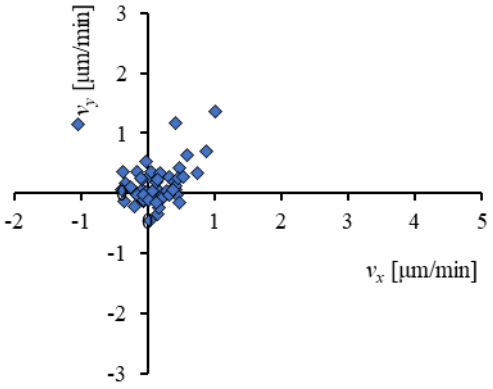

Fig. 8a: Migration velocity before proliferation of C2C12 under shear stress field of 1.5 Pa.

4. DISCUSSION

Endothelial cells are exposed to the shear flow in the blood vessels *in vivo*. The effect of shear flow on endothelial cells was investigated in the previous studies [3−10]. Cells are exfoliated under the shear flow at the wall shear stress higher than 2 Pa [16, 19]. A biological cell shows passive and active responses in an environment [14]. While the flow enhances the cell migration downstream, a cell migrates to adapt to the shear field. While the strong stimulation above the threshold damages the cell, the stimulation below the threshold remains in the cell as a memory for the response in the next step [14]. The hysteresis effect governs the active response of the cell.

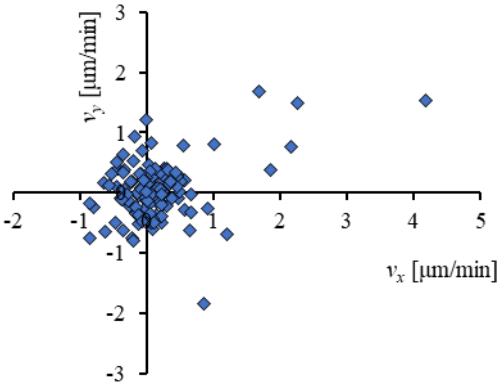

Fig. 8b: Migration velocity after proliferation of C2C12 under shear stress field of 1.5 Pa.

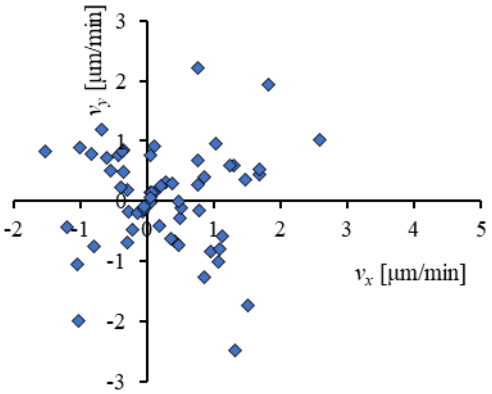

Fig. 9a: Migration velocity before proliferation of HUVEC under shear stress field of 0.9 Pa.

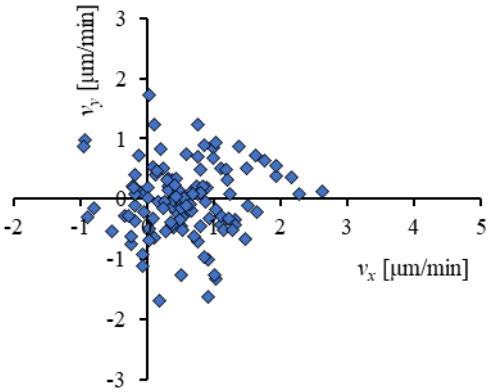

Fig. 9b: Migration velocity after proliferation of HUVEC under shear stress field of 0.9 Pa.

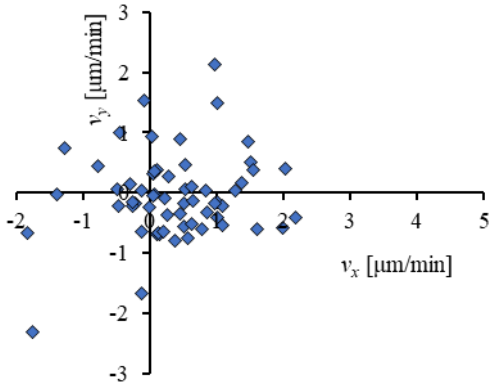

Fig. 10a: Migration velocity before proliferation of HUVEC under shear stress field of 2 Pa.

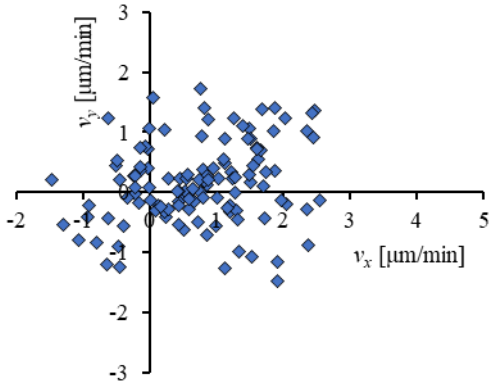

Fig. 10b: Migration velocity after proliferation of HUVEC under shear stress field of 2 Pa.

In the previous study, cells were exposed to the shear flow in a donut-shaped open channel, and the effect of flow stimulation on cultured cells has been studied *in vitro* [15, 24]. When the flow has an open surface, it is difficult to estimate the shear stress value in the fluid. Between two parallel walls, on the other hand, the velocity profile is estimated to be parabolic in the laminar flow. In the previous studies, several preparations were designed to study the effect of mechanical flow stimulations on biological cells: the tilting parallel-walls channel [16], the rhombus channel [17], the cross flow channel [18], and the rotating disk type [20, 21].

The Couette type of flow is convenient to estimate the shear stress in the flow with the constant shear rate between the moving wall and the stationary wall, which is also available to non-Newtonian fluid. The cone-and -plate type device has the uniform shear field in the entire space between the rotating cone and the stationary plate [10, 19]. The shear stress is constant independent of the distance from the rotating axis. The combination of the rotating concave cone and the stationary convex cone is effective to reduce the inertial secondary flow [22].

A parallel disks system between rotating disk and the stationary disk [20, 21], on the other hand, has several advantages: stability of the rotating motion of the disk, stability of the optical path for the microscopic observation, morphologic preciseness of the plane of the disks, and simultaneous observation over the range of variation of the shear rate proportional to the radius from the rotational axis. The behavior of cells under the gradient of the shear stress field can be observed [9,11−13]. The floating erythrocyte deformation was observed between counter rotating parallel discs [23].

In the present study, the rotating parallel disk system is selected to make Couette type of flow instead of the cone and plate system. The rotating flow can induce the secondary flow by the centrifugal effect. The rotational speed of the disk is smaller than 0.4 m s^{-1} in the present system. The microscopic video image of the moving cells between the rotating disk and the stationary disk shows the steady flow in the present experiment. Reynolds number (*Re*) is calculated by Eq. (3).

$$Re = \rho\, v\, d / \eta = \rho\, r\, \omega\, d / \eta \tag{3}$$

In Eq. (3), ρ is density of the fluid, v is the circumferential velocity, r is the distance from the rotating axis, ω is the angular velocity, d is the distance between the moving wall and the stationary wall, and η is the viscosity of the fluid. *Re* is 1.5×10^2, when ρ, r, ω, d, and η are 1×10^3 kg m^{-3}, 18 mm, 22 rad s^{-1}, 0.56 mm, and 1.5×10^{-3} Pa s, respectively. Generation of the turbulent flow is suppressed in the flow at the small value of Reynolds number.

The interaction between cells also governs the behavior of each cell. The migration of each cell depends also on the position of the neighbor cell. Cells are sparsely seeded in the present study. Myoblasts tend to migrate to the oblique direction of the lower shear stress field at 1 Pa. The effect of shear flow on cells depends on the cell types [24, 25]. The dependency can be applied to the cell sorting technology. The quantitative relationships between the shear stress and the cell orientation can be applied to tissue technology to control of cells *in vitro*.

The migration of a biological cell relates to adhesion to the scaffold [1−3]. Cell tends to be rounded at proliferation. In the present experiment *in vitro*, the area (*S*) of the attachment to the scaffold is small during proliferation.

5. CONCLUSION

The effect of shear stress on cell migration has been investigated under Couette type shear flow between parallel disks *in vitro*. HUVEC tends to migrate downstream. The tendency is remarkable after proliferation. Migration tends to be enhanced, when the adhesion area decreased at proliferation. Under the shear stress field (> 1 Pa), C2C12 tend to migrate to the lower shear stress area. The velocity of the migration tends to be higher at HUVEC than C2C12. The experimental system is useful to study the quantitative relationships between the shear stress and the cell migration.

ACKNOWLEDGMENT

The authors thank to Mr. Hiromi Sugimoto for his assistance of the experiment.

REFERENCES

[1] Y.S. Lin, W. Liu and C. Hu, "Investigation of Cells Migration Effects in Microfluidic Chips", **Journal of Chromatography Separation Techniques**, Vol. 8, No. 1, 2017. P. 345.

[2] S. Chung, R. Sudo, P.J. Mack, C.R. Wan, V. Vickerman and R.D. Kamm, "Cell Migration into Scaffolds under Co-culture Conditions in a Microfluidic Platform", **Lab on a Chip**, Vol. 9, No. 2, 2009, pp. 269−275.

[3] M.A. Ostrowski, N.F. Huang, T.W. Walker, T. Verwijlen, C. Poplawski, A.S. Khoo, J.P. Cooke, G.G. Fuller and A.R. Dunn, "Microvascular Endothelial Cells Migrate Upstream and Align Against the Shear Stress Field Created by Impinging Flow", **Biophysical Journal**, Vol. 106, No. 2, 2014, pp. 366–374.

[4] M.J. Levesque and R.M. Nerem, "The Elongation and Orientation of Cultured Endothelial Cells in Response to Shear Stress", **Journal of Biomechanical Engineering**, Vol. 107, No. 4, 1985, pp. 341−347.

[5] R. Steward Jr, D. Tambe, C.C. Hardin, R. Krishnan and J.J. Fredberg, "Fluid Shear, Intercellular Stress, and Endothelial Cell Alignment", **American Journal of Physiology–Cell Physiology**, Vol. 308, 2015, C657–C664.

[6] T. Nagel, N. Resnick, W.J. Atkinson, C.F. Dewey Jr and M. A. Gimbrone Jr, "Shear Stress Selectively Upregulates Intercellular Adhesion Molecule-1 Expression in Cultured Human Vascular Endothelial Cells", **The Journal of Clinical Investigation**, Vol. 94, No. 2, 1994, pp. 885–891.

[7] N. Kataoka, S. Ujita and M.Sato, "Effect of Flow Direction on the Morphological Responses of Cultured Bovine Aortic Endothelial Cells", **Medical & Biological Engineering & Computing**, Vol. 36, 1998, pp. 122−128.

[8] N. Sakamoto and N. Saito, "Effect of Spatial Gradient in Fluid Shear Stress on Morphological Changes in Endothelial Cells in Response to Flow", **Biochemical and Biophysical Research Communications**, Vol. 395, 2010, pp. 264−269.

[9] C.R. White, M. Haidekker, X. Bao and J.A. Frangos, "Temporal Gradients in Shear, but Not Spatial Gradients, Stimulate Endothelial Cell Proliferation", **Circulation**, Vol. 103, 2001, pp. 2508−2513.

[10] M.H. Buschmann, P. Dieterich, N.A. Adams and H.J. Schnittler, "Analysis of Flow in a Cone-and-plate Apparatus with Respect to Spatial and Temporal Effects on Endothelial Cells", **Biotechnology and Bioengineering**, Vol. 89, No. 55, 2005, pp. 493−502.

[11] N. DePaola, M.A. Gimbrone Jr., P.F. Davies and C.F. Dewey Jr., "Vascular Endothelium Responds to Fluid Shear Stress Gradients", **Arteriosclerosis Thrombosis and Vascular Biology**, Vol 12, No 11, 1992, pp. 1254−1257.

[12] Y. Tardy, N. Resnick, T. Nagel, M.A. Gimbrone Jr and C.F. Dewey Jr, "Shear Stress Gradients Remodel Endothelial Monolayers in Vitro via a Cell Proliferation-Migration-Loss Cycle", **Arteriosclerosis Thrombosis and Vascular Biology**, Vol. 17, No. 11, 1997, pp. 3102–3106.

[13] J.M. Dolan, H. Meng, S. Singh, R. Paluch and J. Kolega, "High Fluid Shear Stress and Spatial Shear Stress Gradients Affect Endothelial Proliferation, Survival, and Alignment", **Annals of Biomedical Engineering**, Vol. 39, No.6, 2011, pp. 1620−1631.

[14] R.H.W. Lam, Y. Sun, W. Chen and J. Fu, "Elastomeric Microposts Integrated into Microfluidics for Flow-mediated Endothelial Mechanotransduction Analysis", **Lab on a Chip**, Vol. 12, No. 10, 2012, pp. 1865−1873.

[15] S. Hashimoto and M. Okada, "Orientation of Cells Cultured in Vortex Flow with Swinging Plate In Vitro", **Journal of Systemics Cybernetics and Informatics**, Vol. 9, No. 3, 2011, pp. 1−7.

[16] S. Hashimoto, F. Sato, H. Hino, H. Fujie, H. Iwata and Y. Sakatani, "Responses of Cells to Flow In Vitro", **Journal of Systemics Cybernetics and Informatics**, Vol. 11, No. 5, 2013, pp. 20−27.

[17] F. Sato, S. Hashimoto, T. Yasuda and H. Fujie, "Observation of Biological Cells in Rhombus Parallelepiped Flow Channel", **Proc. 17th World Multi-Conference on Systemics Cybernetics and Informatics**, Vol. 1, 2013, pp. 25−30.

[18] H. Hino, S. Hashimoto, Y. Takahashi and S. Nakano, "Design of Cross Type of Flow Channel to Control Orientation of Cell", **Proc. 20th World Multi-Conference on Systemics Cybernetics and Informatics**, Vol. 2, 2016, pp. 117−122.

[19] S. Hashimoto, H. Sugimoto and H. Hino, "Behavior of Cell in Uniform Shear Flow Field between Rotating Cone and Stationary Plate", **Journal of Systemics Cybernetics and Informatics**, Vol. 16, No. 2, 2018, pp. 1−7.

[20] H. Hino, S. Hashimoto, Y. Takahashi and M. Ochiai, "Effect of Shear Stress in Flow on Cultured Cell: Using Rotating Disk at Microscope", **Journal of Systemics, Cybernetics and Informatics**, Vol. 14, No. 4, 2016, pp. 6−12.

[21] S. Hashimoto, H. Sugimoto and H. Hino, "Effect of Couette Type of Shear Stress Field with Axial Shear Slope on Deformation and Migration of Cell: Comparison Between C2C12 and HUVEC", **Journal of Systemics Cybernetics and Informatics**, Vol. 17, No. 2, 2019, pp. 4−10.

[22] S. Hashimoto, "Erythrocyte Destruction under Periodically Fluctuating Shear Rate; Comparative Study with Constant Shear Rate", **Artificial Organs**, Vol. 13, No. 5, 1989, pp. 458−463.

[23] S. Hashimoto, "Detect of Sublethal Damage with Cyclic Deformation of Erythrocyte in Shear Flow", **Journal of Systemics Cybernetics and Informatics**, Vol. 12, No. 3, 2014, pp. 41−46.

[24] M. Ochiai, S. Hashimoto and Y. Takahashi, "Effect of Flow Stimulation on Cultured Osteoblast", **Proc. 18th World Multi-Conference on Systemics Cybernetics and Informatics**, Vol. 2, 2014, pp. 156−161.

[25] W. Yu, H. Qu, G. Hu, Q. Zhang, K. Song, H. Guan, T. Liu and J. Qin, "A Microfluidic-based Multi-shear Device for Investigating the Effects of Low Fluid-induced Stresses on Osteoblasts", **PLoS ONE**, Vol. 9, No. 2, 2014, pp. 1−7.